

University of Sheffield

# Integrated Navigation for Aircraft: ACS6124

## Multisensor Report



Mafaz Syed (200118234)

*Lecturer:* Dr Yuanbo Nie

A report submitted in partial fulfilment of the requirements  
for the Multisensor Assignment for the Multisensor and Decision Systems Module (ACS6124)

*in the*

Automatic Control and Systems Engineering Department

May 9, 2024

# Contents

<b>1 Task 1: Kalman Filter Design</b>	<b>1</b>
1.1 Task 1.1: Derivation of Jacobian Matrices . . . . .	1
1.1.1 F Matrix . . . . .	1
1.1.2 G Matrix . . . . .	1
1.1.3 H Matrix . . . . .	1
1.2 Task 1.2: Implementation and Evaluation of the Kalman Filter . . . . .	1
1.2.1 Trajectories of the Estimated States . . . . .	1
<b>2 Task 2: Removing Sensor Biases</b>	<b>2</b>
2.1 Task 2.1: Comparison of Trajectories with and without Sensor Biases . . . . .	2
2.1.1 Comparison of Estimated Trajectories with and without Bias . . . . .	2
2.1.2 Discussion on the Degradation in Estimation Performance . . . . .	3
2.2 Task 2.2: Estimation with Bias Compensation . . . . .	4
<b>3 Task 3: Sensor Fault Detection and Diagnosis</b>	<b>7</b>
3.1 Task 3.1: Fault Detection using Kalman Filter Innovations . . . . .	7
3.1.1 History of the Innovation of the Extended Kalman Filter . . . . .	7
3.1.2 Rationales Behind the Use of KF Innovation for Fault Detection . . . . .	7
3.2 Task 3.2: Fault Mitigation . . . . .	8
3.3 Task 3.3: Fault Detection Scheme Design and Trade-offs . . . . .	11
3.4 Task 3.4: Detection and Mitigation of Cyber Attack on Sensor Readings . . . . .	14

## List of Figures

1	Trajectories of the Estimated States after Kalman Filter Implementation . . . . .	2
2	State Estimation after Kalman Filter Comparing Biased and Unbiased Datasets (solid red line and dotted blue line); Variables with the most pronounced effects highlighted in a green box. . . . .	3
3	Estimated Trajectories of States after Bias Mitigation . . . . .	5
4	Bias Convergence after Bias Mitigation Implemented on State Estimation . . . . .	6
5	Innovation History of EKF (dataTask3_1.mat). First sensor fault occurs at step 3 (around 45 seconds). . . . .	7
6	Estimated State Trajectories Compared After Fault Mitigation Compared and Before Fault Mitigation . . . . .	9
7	Innovation After Fault Mitigation Compared with Innovation Before Fault Mitigation	10
8	Faults in Bias Estimates . . . . .	11
9	CUSUM Test for Time Estimation for Bias Faults . . . . .	12
10	Faults in Bias Estimates with Time Instance (Obtained from CUSUM Test) . . . . .	13
11	Fault Time Instance for Angle of Attack (From CUSUM Test) . . . . .	14
12	Innovation Comparison of AoA with and without Fault Mitigation . . . . .	15
13	Estimated State Trajectories after Cyber Attack Mitigation . . . . .	15

# 1 Task 1: Kalman Filter Design

## 1.1 Task 1.1: Derivation of Jacobian Matrices

For the design of the integrated GPS/IMU/Air-data navigation system, the Kalman filter requires the derivation of Jacobian matrices. These matrices are critical for updating the state estimate and error covariance in response to new measurements.

Given the nonlinear nature of our system, the Jacobian matrices  $F$ ,  $G$ , and  $H$  are utilised which represent the partial derivatives of the system dynamics and measurement models with respect to the state variables and noise terms. The matrices  $F$ ,  $G$ , and  $H$  are defined by  $\frac{\partial f}{\partial x}$ ,  $\frac{\partial g}{\partial w}$ , and  $\frac{\partial h}{\partial x}$ . The expressions for the desired elements for each matrix are presented below.

### 1.1.1 F Matrix

**5th Row, 4th Column:**

$$F_{54} = -r_m$$

**6th Row, 7th Column:**

$$F_{67} = -g \cos(\theta) \sin(\phi); g = 9.81 \text{m/s}^2$$

### 1.1.2 G Matrix

**4th Row, 6th Column:**

$$G_{46} = -v$$

**9th Row, 5th Column:**

$$G_{95} = -\frac{\sin(\phi)}{\cos(\theta)}$$

### 1.1.3 H Matrix

**7th Row, 7th Column:**

$$H_{77} = 1$$

**11th Row, 4th Column:**

$$H_{14} = -\frac{w}{u^2 \left( \frac{w^2}{u^2} + 1 \right)}$$

## 1.2 Task 1.2: Implementation and Evaluation of the Kalman Filter

### 1.2.1 Trajectories of the Estimated States

The estimated trajectories of the 12 states, which include the position ( $x_E$ ,  $y_E$ , and  $z_E$ ), velocity ( $u$ ,  $v$ , and  $w$ ), attitude ( $\phi$ ,  $\theta$ , and  $\psi$ ), and the wind velocities ( $V_{wxE}$ ,  $V_{wyE}$ , and  $V_{wxE}$ ), of the navigation system were obtained by implementing the Kalman Filter algorithm, and using the derived Jacobian matrices.

The estimated trajectories are plotted in Figure 1 to provide visual insights into the behavior of navigation system over time.

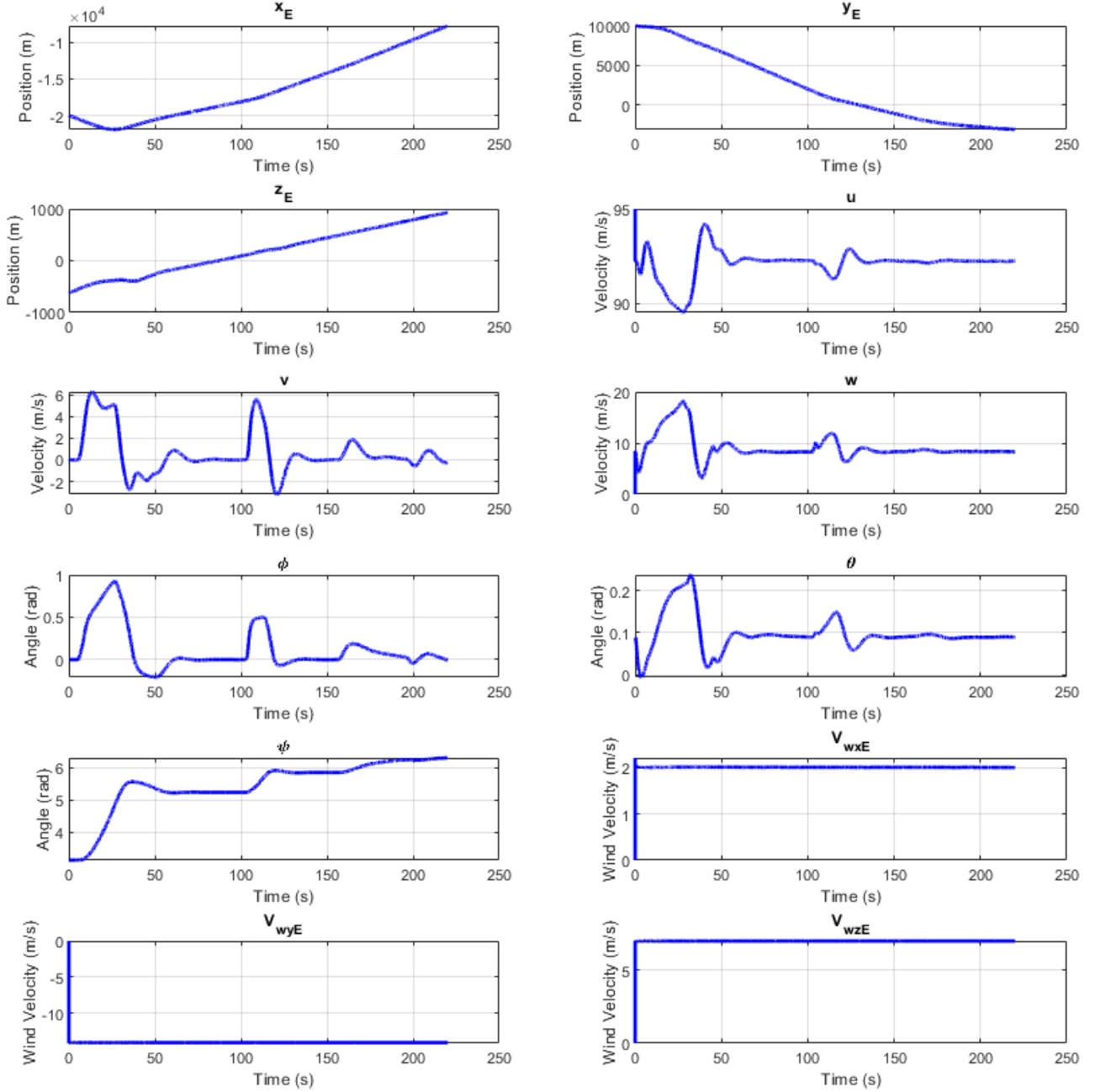


**Figure 1:** Trajectories of the Estimated States after Kalman Filter Implementation

## 2 Task 2: Removing Sensor Biases

### 2.1 Task 2.1: Comparison of Trajectories with and without Sensor Biases

The trajectories of the estimated states obtained from Task 1 (using unbiased data) were compared with those from Task 2, which re-runs Task 1 using `dataTask2.mat` that includes IMU sensor biases.

#### 2.1.1 Comparison of Estimated Trajectories with and without Bias

The comparison of the state trajectories between Task 1 (blue dashed line) and Task 2 (red solid line) is visualised in Figure 2; variables with the most pronounced differences ( $u, v, w, \theta, V_{wxE}$ , and  $V_{wzE}$ ) are highlighted with a green box.

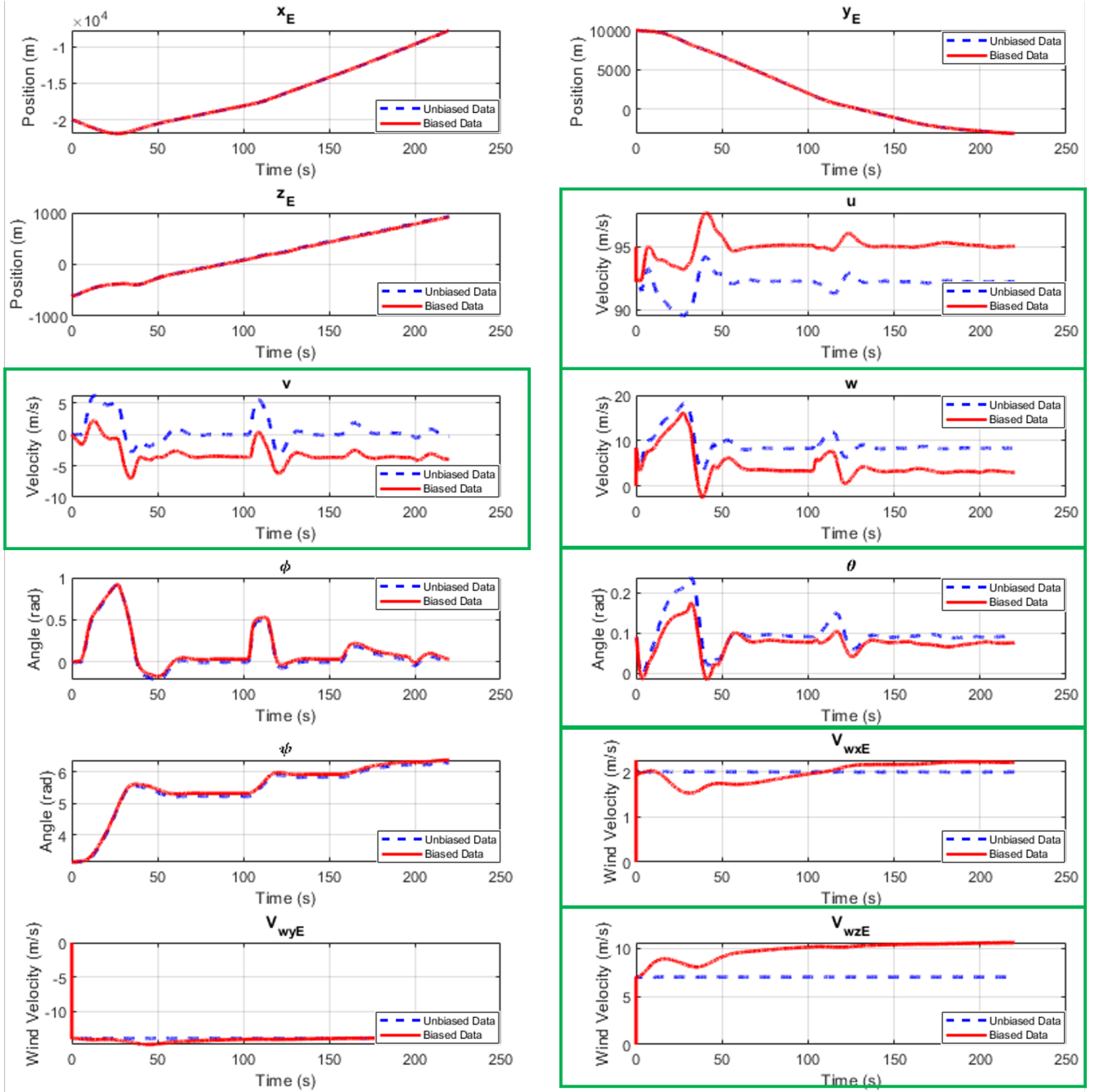


**Figure 2:** State Estimation after Kalman Filter Comparing Biased and Unbiased Datasets (solid red line and dotted blue line); Variables with the most pronounced effects highlighted in a green box.

### 2.1.2 Discussion on the Degradation in Estimation Performance

**Magnetometer and Anemometer Issues:** The magnetometer, used for measuring the Earth's magnetic field, is susceptible to interference from the aircraft's electronics, magnetic fields at the equator and poles (1), and turbulence (2) (3). The anemometer, used to measure wind speed, can develop biases due to turbulence (4) and wind gusts (or self-excited air turbulence (5)) (6).

**Sensor Bias Accumulation:** IMU biases, particularly gyroscopic biases (7), accumulate over time, leading to systematic errors in attitude estimation (8). The body velocity components ( $u, v, w$ ) directly depend on accurate attitude estimates. Therefore, errors in attitude estimation propagate to the velocity estimates.

**Cascading Effect:** Errors in attitude estimation cause incorrect transformations of body velocities to the Earth reference frame (9). This cascading effect results in inaccurate wind velocity estimates due to incorrect subtraction of body velocities (10). The following paper (11) looks deeper into cascaded Kalman filters for accurate estimation of these biases.

**Impact on Kalman Filter:** The Kalman filter assumes uncorrelated noise (12). However, systematic biases violate this assumption (13), leading to residuals (innovations) that are not purely Gaussian, which degrades the filter's estimation performance.

**Gyroscopic Bias:** Gyroscopes in IMUs are prone to biases and drifts over time, as well as sensor aging (14) (15). The presence of biases leads to systematic errors in the gyroscope measurements, which significantly impact attitude estimation (16).

Sensor biases cause a significant degradation in estimation performance due to the propagation of errors across attitude and velocity states. Correcting these biases is important for accurate state estimation, which will be addressed in Task 2.2 by modifying the Kalman filter to explicitly estimate the biases alongside the state variables.

## 2.2 Task 2.2: Estimation with Bias Compensation

In this task, the state estimation model was extended to include sensor biases as part of the state vector and the kalman filter was used to estimate both the states and the biases. The accuracy and reliability of the navigation system was enhanced by effectively removing sensor biases and improving the estimation performance of the Kalman filter.

The original state vector was extended to include the biases for accelerometer and gyroscopes, as shown in Equation 1:

$$x = [x_E, y_E, z_E, u, v, w, \phi, \theta, \psi, b_{Ax}, b_{Ay}, b_{Az}, b_p, b_q, b_r, V_{wxE}, V_{wyE}, V_{wzE}] \quad (1)$$

The kinematic equations were updated to include the biases. The state matrices  $F$ ,  $G$ , and  $H$  were updated to reflect the augmented state vector. The Kalman filter was executed using the new model to estimate both the states and biases.

Figure 3 shows the estimated state trajectories for comparison with and without bias mitigation. Figure 4 shows the estimated bias for accelerometer ( $b_{Ax}, b_{Ay}, b_{Az}$ ) and gyroscopes ( $b_p, b_q, b_r$ ) over time.

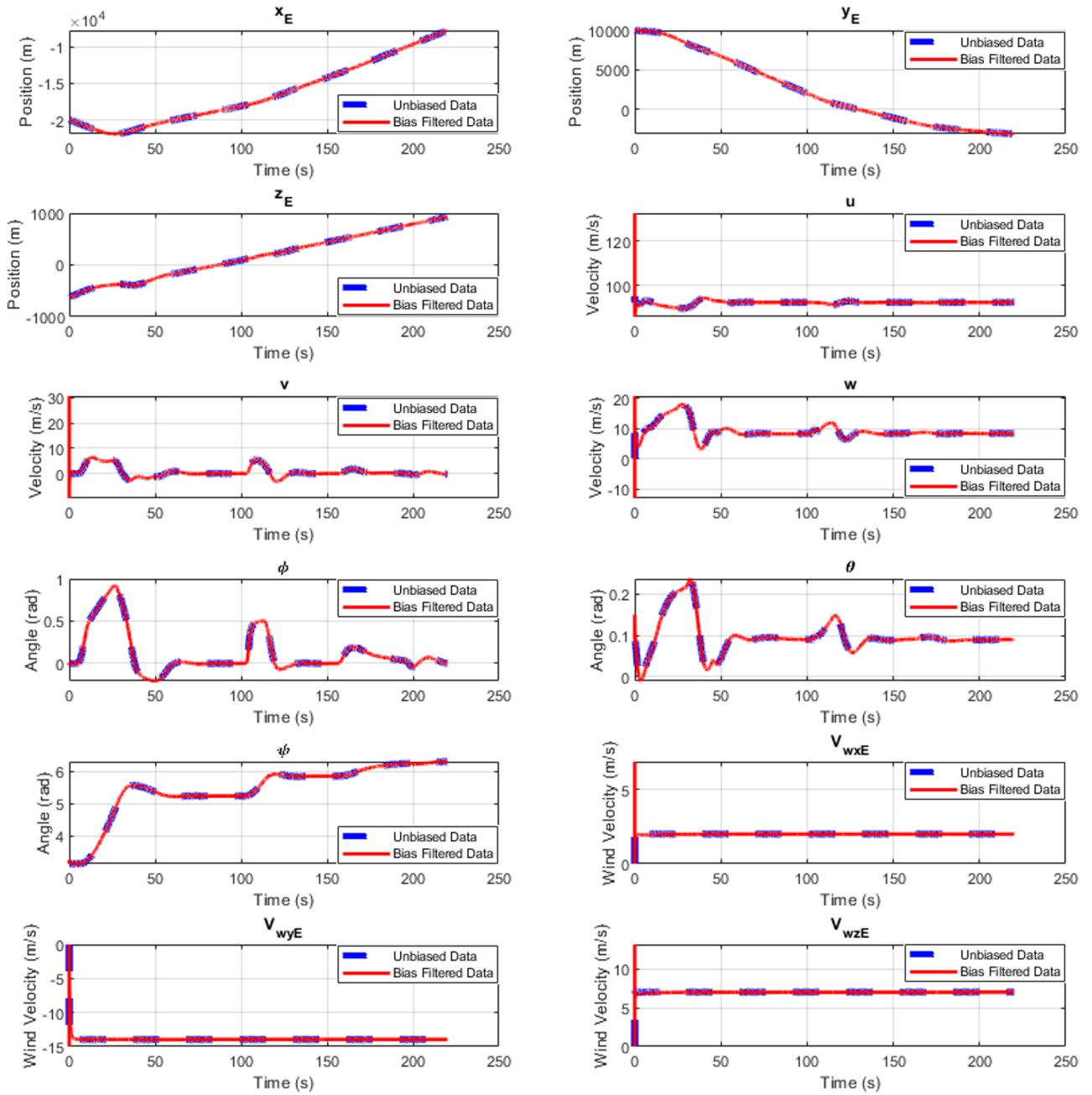


**Figure 3:** Estimated Trajectories of States after Bias Mitigation

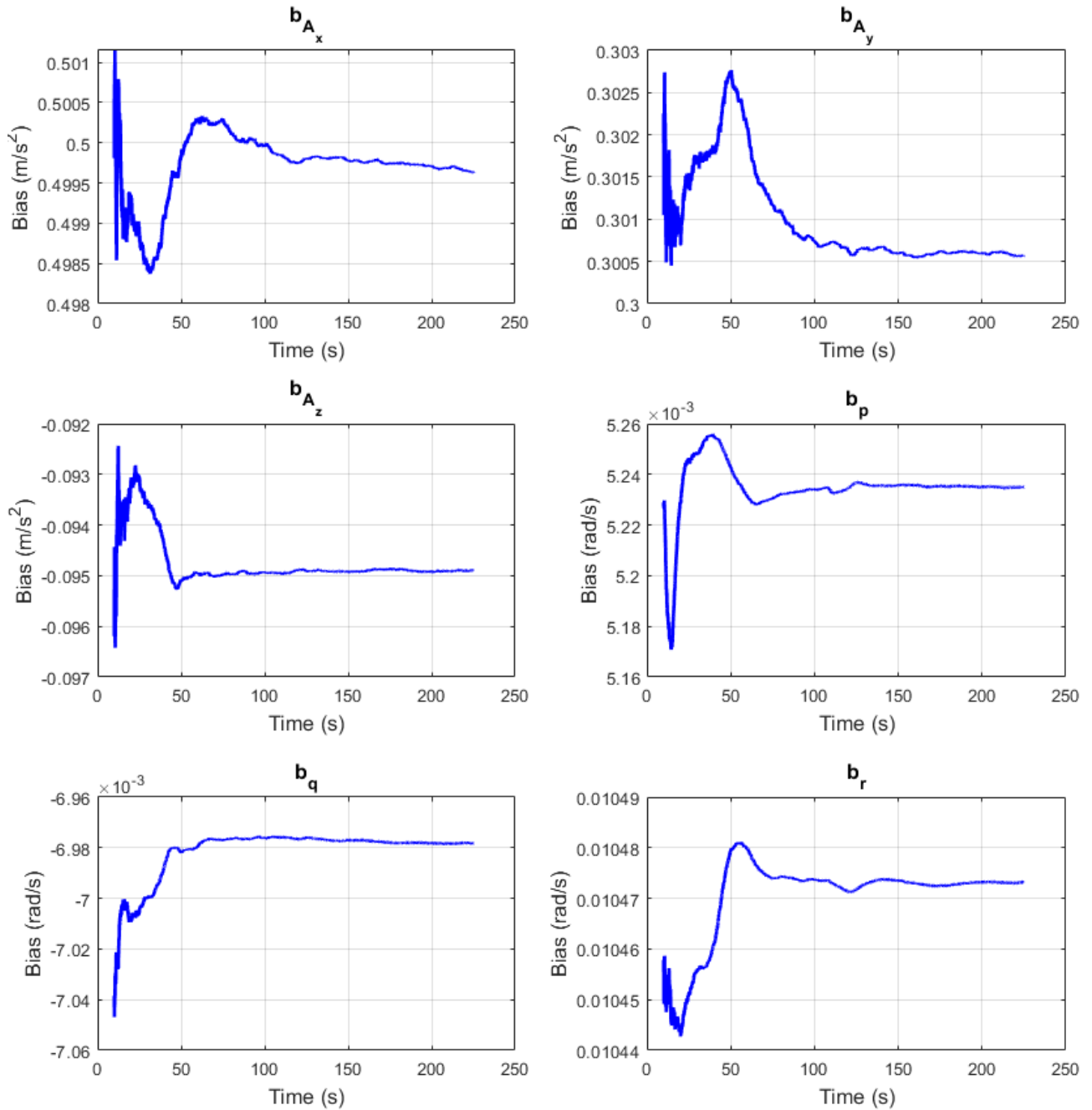


**Figure 4:** Bias Convergence after Bias Mitigation Implemented on State Estimation

### 3 Task 3: Sensor Fault Detection and Diagnosis

#### 3.1 Task 3.1: Fault Detection using Kalman Filter Innovations

##### 3.1.1 History of the Innovation of the Extended Kalman Filter

In this task, the innovation history of the Extended Kalman Filter (EKF) is analysed to detect and diagnose sensor faults using the data provided in `dataTask3_1.mat`.

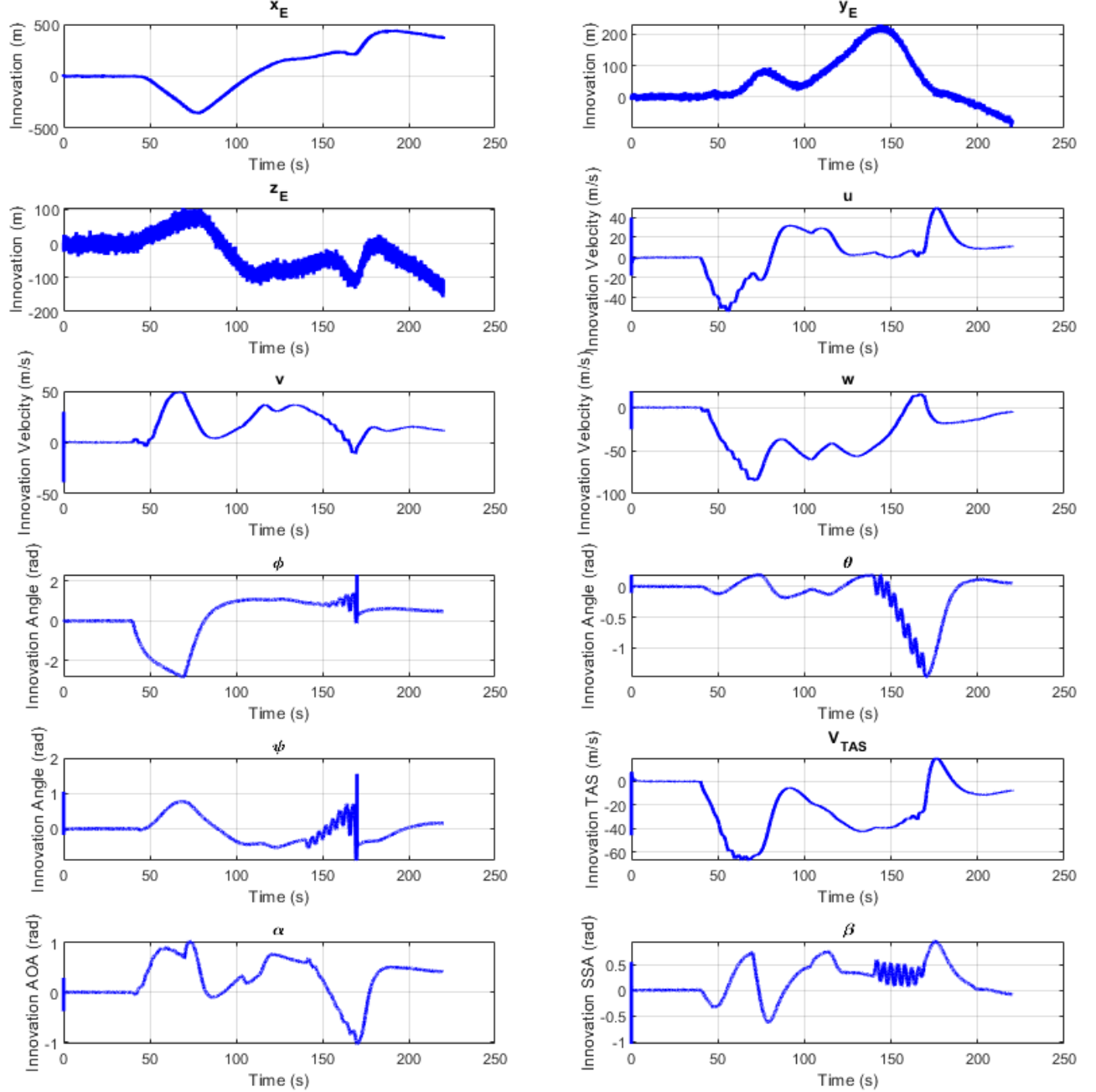


**Figure 5:** Innovation History of EKF (`dataTask3_1.mat`). First sensor fault occurs at step 3 (around 45 seconds).

##### 3.1.2 Rationales Behind the Use of KF Innovation for Fault Detection

The rationale behind using Kalman filter innovation for fault detection lies in its sensitivity to discrepancies between expected and actual sensor outputs (17). The innovation sequence effectively

highlights discrepancies caused by sensor faults, making it a valuable diagnostic tool in fault detection and diagnosis (FDD) systems (18).

**Definition of Innovation:** Innovation (or residual) is the difference between the actual (observed) measurement and the predicted measurement based on the current state estimate (19) (20), as depicted in Equation 2:

$$innov(k,:) = z_k(k,:) - \hat{z}_k \quad (2)$$

where  $z_k(k,:)$  is the actual measurement vector at time  $k$ , and  $\hat{z}_k$  is the predicted measurement vector based on the state prediction at time  $k$ .

**Properties of Innovation:** In the absence of faults, the innovation should follow a Gaussian distribution centered around zero, assuming correctly estimated noise covariances (20). The innovation covariance matrix  $S$  is given by Equation 3:

$$S = HPH^T + R \quad (3)$$

where  $H$  is the measurement matrix,  $P$  is the state estimation error covariance, and  $R$  is the measurement noise covariance.

**Fault Detection Principle:** A significant deviation in innovation from zero indicates a discrepancy between the predicted and actual measurements, which can signal sensor faults (20). By monitoring the magnitude and pattern of the innovation, the occurrence of sensor faults can be detected (21).

#### Benefits of Innovation Monitoring:

- **Sensitivity:** The filter's sensitivity to specific sensor characteristics allows it to detect subtle faults that may not cause immediate system failures but could lead to degraded performance over time.
- **Real-Time Monitoring:** Real-time monitoring of the innovation provides immediate feedback on system integrity, allowing for prompt corrective actions.

### 3.2 Task 3.2: Fault Mitigation

In this task, 6 additional noise terms representing faults (bias changes) are included and their influence mitigated, as depicted in Equation 4.

$$\omega = [\omega_{Ax}, \omega_{Ay}, \omega_{Az}, \omega_p, \omega_q, \omega_r, \omega_{bAx}, \omega_{bAy}, \omega_{bAz}, \omega_{bP}, \omega_{bq}, \omega_{br}] \quad (4)$$

Figure 6 compares the estimated state trajectories before and after fault mitigation, demonstrating successful convergence and fault mitigation.

Figure 7 presents the innovations before and after fault mitigation. The post-mitigation innovations show a mean close to zero, indicating successful fault mitigation and the system's ability to detect and correct sensor faults effectively.

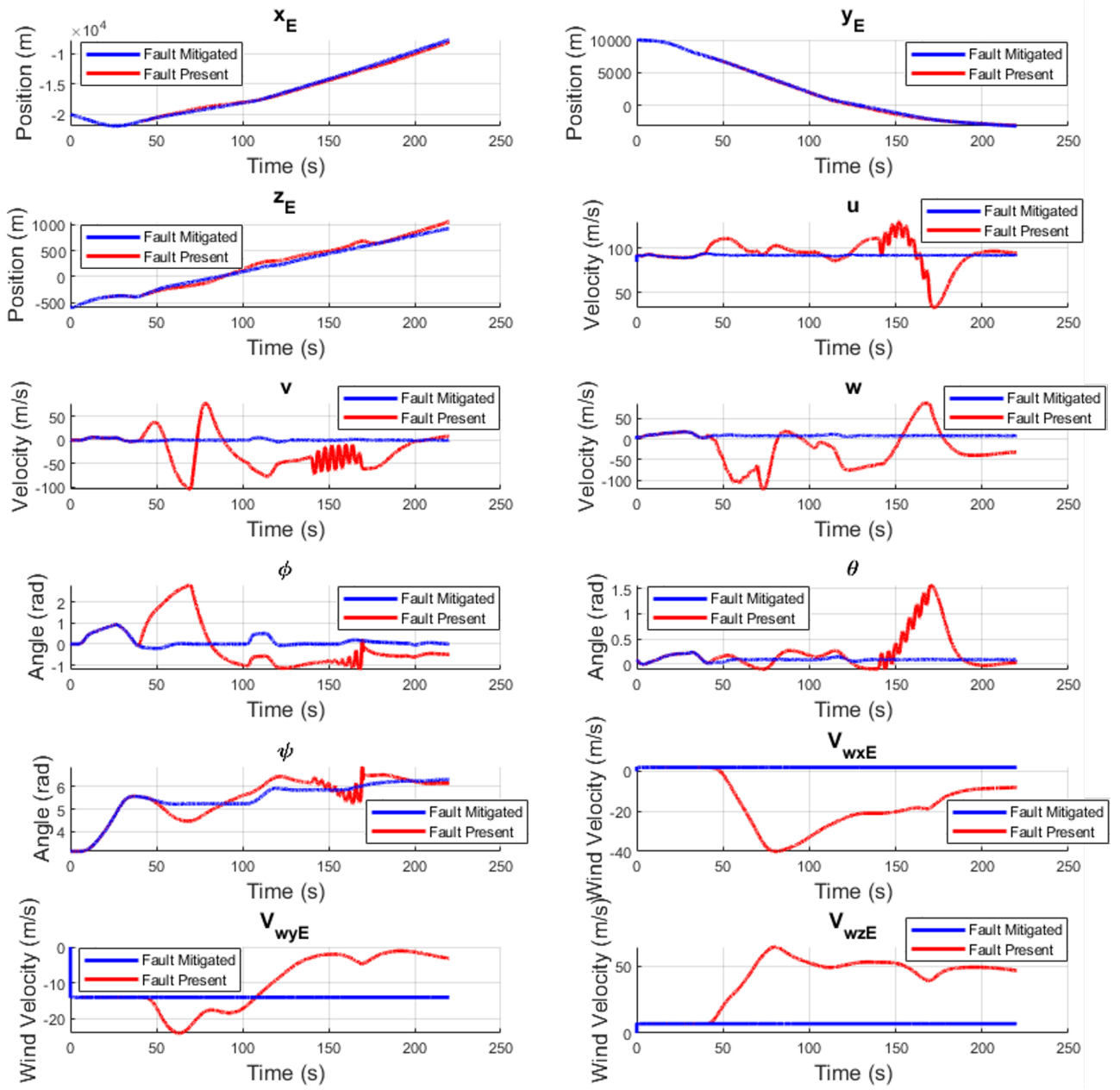


**Figure 6:** Estimated State Trajectories Compared After Fault Mitigation Compared and Before Fault Mitigation

**Fault Mitigation Evidence:** The innovation history after mitigation (red line) shows significantly reduced spikes compared to before mitigation (blue line), confirming successful detection and correction of faults. The initial spikes visible after 45 seconds (observed in Task 3.1) are absent in the updated innovation history.

**Reduced Deviation:** The innovations now remain centered around zero, with fewer deviations exceeding the threshold, indicating a more accurate state estimation.

**Comparison of State Estimations:** The state estimations after fault mitigation show very close convergence to the true trajectory from task 1.

- **Position and Attitude:** The position and attitude estimates show reduced drift and closer convergence to the true trajectory after fault mitigation.
- **Airspeed Body Components:** The body velocity components ( $u, v, w$ ) exhibit smoother

trajectories and better accuracy with bias correction.

- **Wind Velocity Components:** The wind velocity components ( $V_{wxE}$ ,  $V_{wyE}$ ,  $V_{wzE}$ ) show significant improvements in estimation accuracy after fault mitigation, removing large deviations.

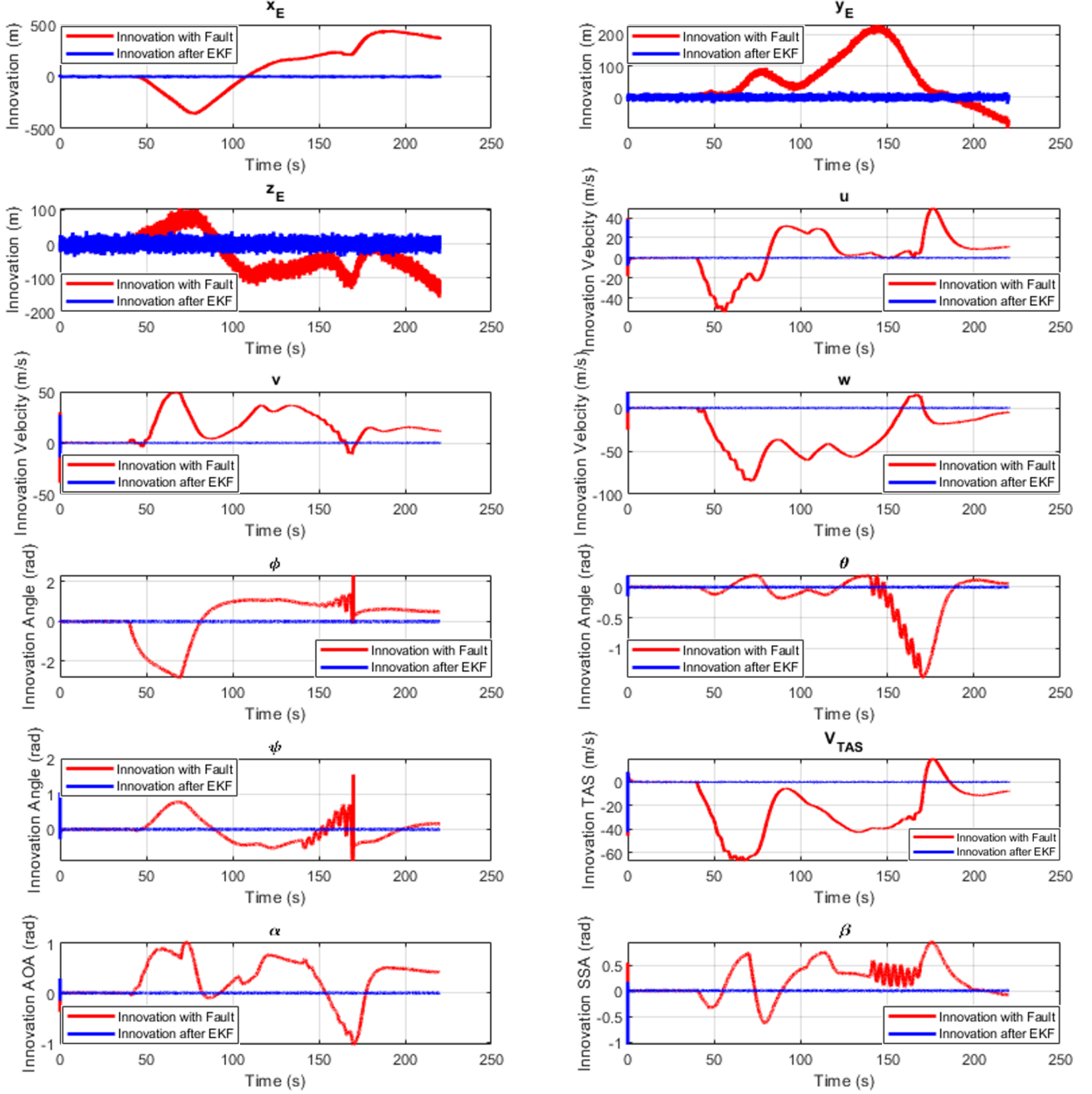


**Figure 7: Innovation After Fault Mitigation Compared with Innovation Before Fault Mitigation**

Updating the navigation model to include fault biases and their noise terms successfully detected and mitigated sensor faults. The innovations showed significant improvements in the fault detection and correction, leading to stabilized state estimates. Additionally, the comparison of state trajectories confirms that fault mitigation significantly improves estimation accuracy and stability.

### 3.3 Task 3.3: Fault Detection Scheme Design and Trade-offs

In this task, the fault onset times in IMU measurements, including accelerometer signals  $A_x$ ,  $A_y$ ,  $A_z$ , and gyroscope signals  $p$ ,  $q$ , and  $r$ , are identified. A two-sided Cumulative Sum (CUSUM) approach (22) is employed due to its inherent benefits.

**Detection of Small Mean Shifts:** It is highly effective in identifying subtle, gradual faults by detecting minor mean shifts in noisy signals that are often overlooked by static threshold monitoring (23). **Memoryless Property:** Enables real-time application in dynamic environments, providing fault detection at every time step.

**Reference Value ( $K$ ):** Controls sensitivity to shifts in innovations. A smaller  $K$  increases detection sensitivity, while a larger  $K$  reduces false alarms but may delay detection of subtle faults.

**Decision Interval ( $h$ ):** Adjusted to balance the trade-off between detection rate and false alarms. A lower  $h$  increases sensitivity but also raises false alarms.

**Reduction of State Estimation Uncertainty:** Incorporating the biases' structure improves the precision of their corresponding state estimates.

**Robustness to False Positives/Negatives:** Differentiating between faulty and non-faulty states minimizes false positives and negatives.

In Figures 8 to 10, the detection of faults in the six states is evident. Notably, no fault is detected in the  $A_y$  state. The clear time instances of faults in other states are shown, and these values are plotted over the original bias estimates.

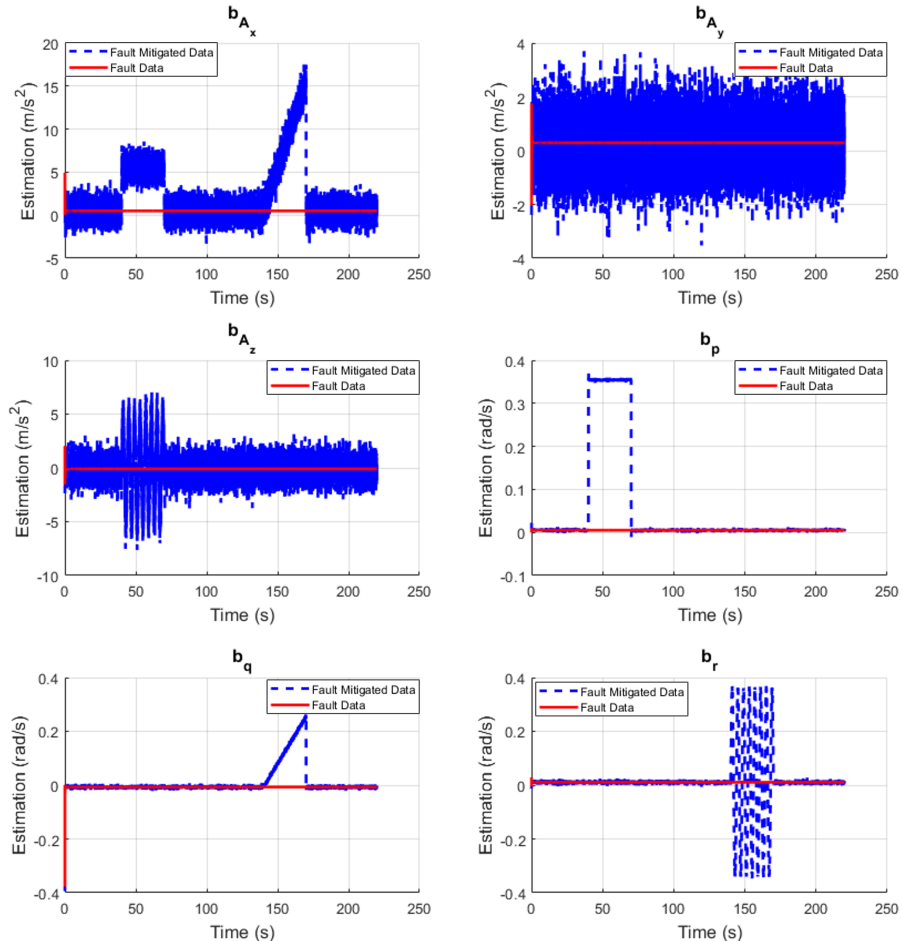
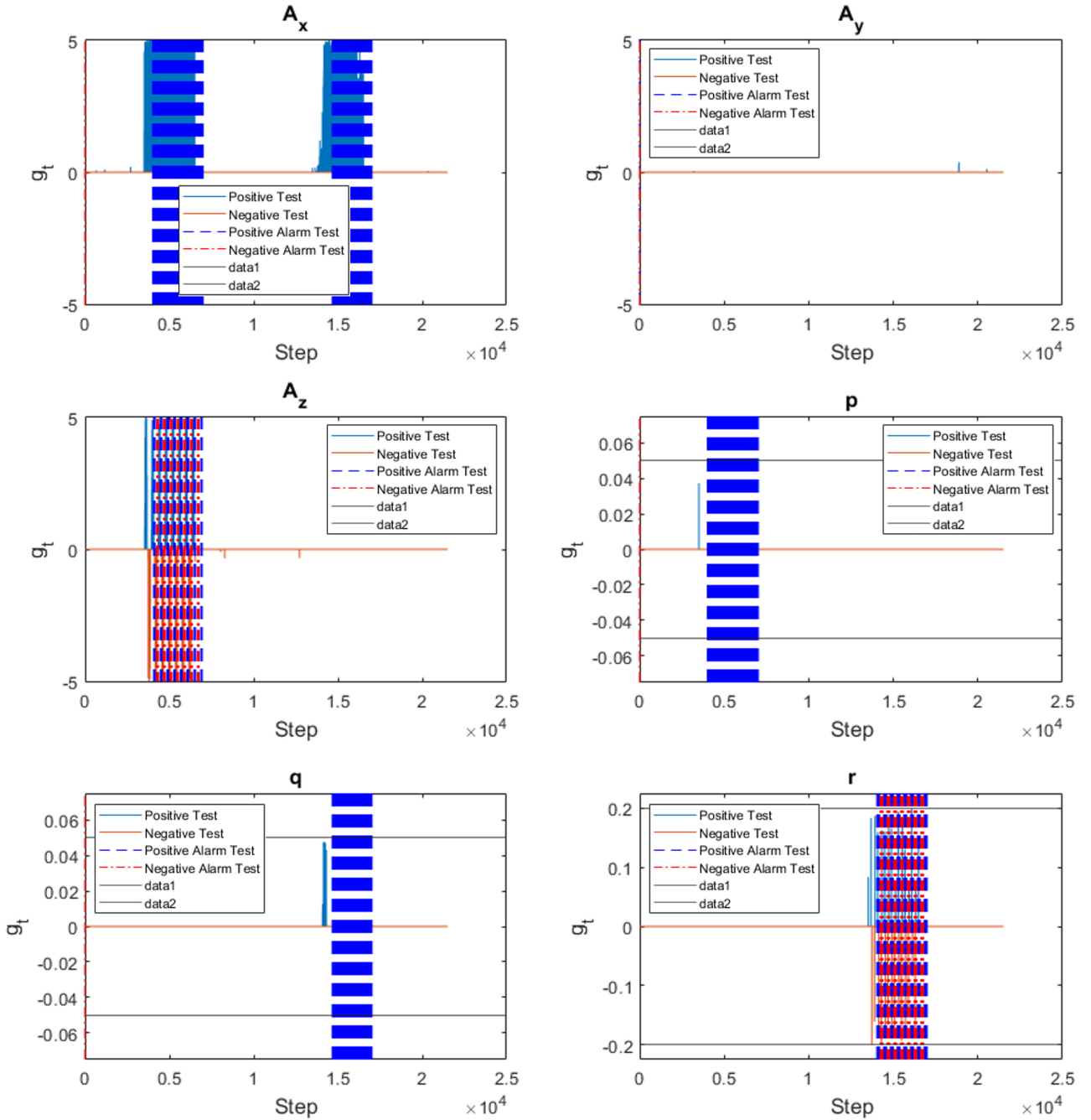
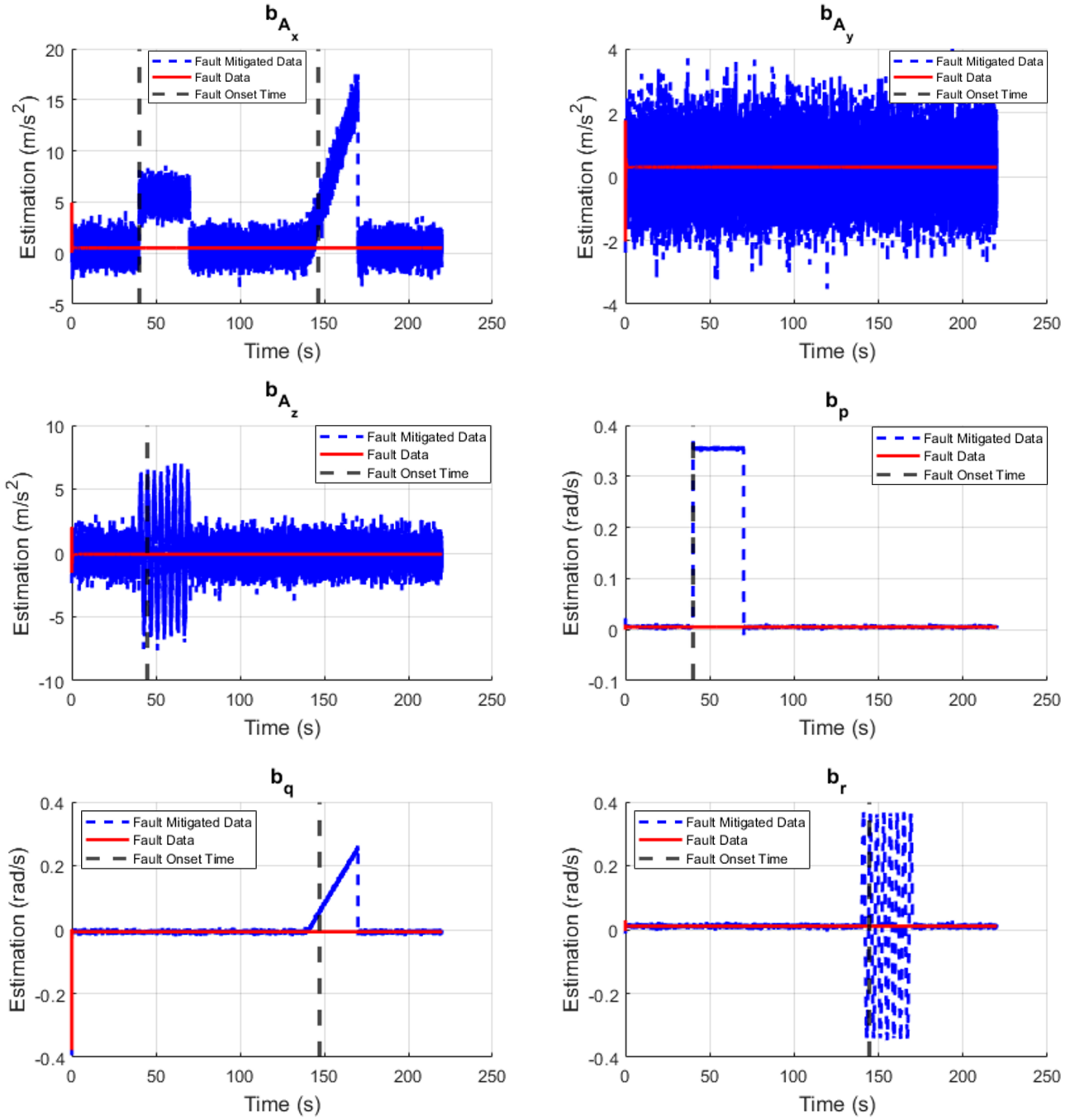


Figure 8: Faults in Bias Estimates



**Figure 9:** CUSUM Test for Time Estimation for Bias Faults

The CUSUM test accumulates deviations over time, enabling quicker and more reliable detection of gradual faults than static threshold monitoring. A slightly higher false alarm rate is acceptable to ensure prompt fault detection, crucial for aircraft safety. Minimizing false alarms reduces unnecessary maintenance and operational interruptions. Bias oscillations typically settle after 5 seconds, filtering out false positives. Setting leaks and thresholds based on state peaks improves robustness. MATLAB's `ischange()` function helps identify discontinuities.



**Figure 10:** Faults in Bias Estimates with Time Instance (Obtained from CUSUM Test)

### 3.4 Task 3.4: Detection and Mitigation of Cyber Attack on Sensor Readings

Enhanced Fault Detection Design: A combination of standardized innovation analysis and a CUSUM test is used to identify and mitigate tampering with the  $\alpha$  sensor.

#### Standardised Innovation Analysis:

- Measure the standardised innovation against a known variance factor.
- If the innovation of  $\alpha$  exceeds the threshold, the measurement is discarded, and the innovation is set to zero.

#### Justification for the Choice of Fault Detection Scheme:

- Standardised Innovation Analysis:

- Standardizing the innovation against a known variance factor provides a robust method to identify faulty measurements.
- Discarding faulty measurements ensures accurate state estimation.

- CUSUM Test Effectiveness:

- Detects subtle shifts in the innovation of the  $\alpha$  sensor quickly and efficiently.
- Useful for identifying cyberattacks that inject false signals.

Figure 11 to Figure 13 show the fault time instance for the angle of attack, innovation, and the estimated state trajectories after cyber attack mitigation.

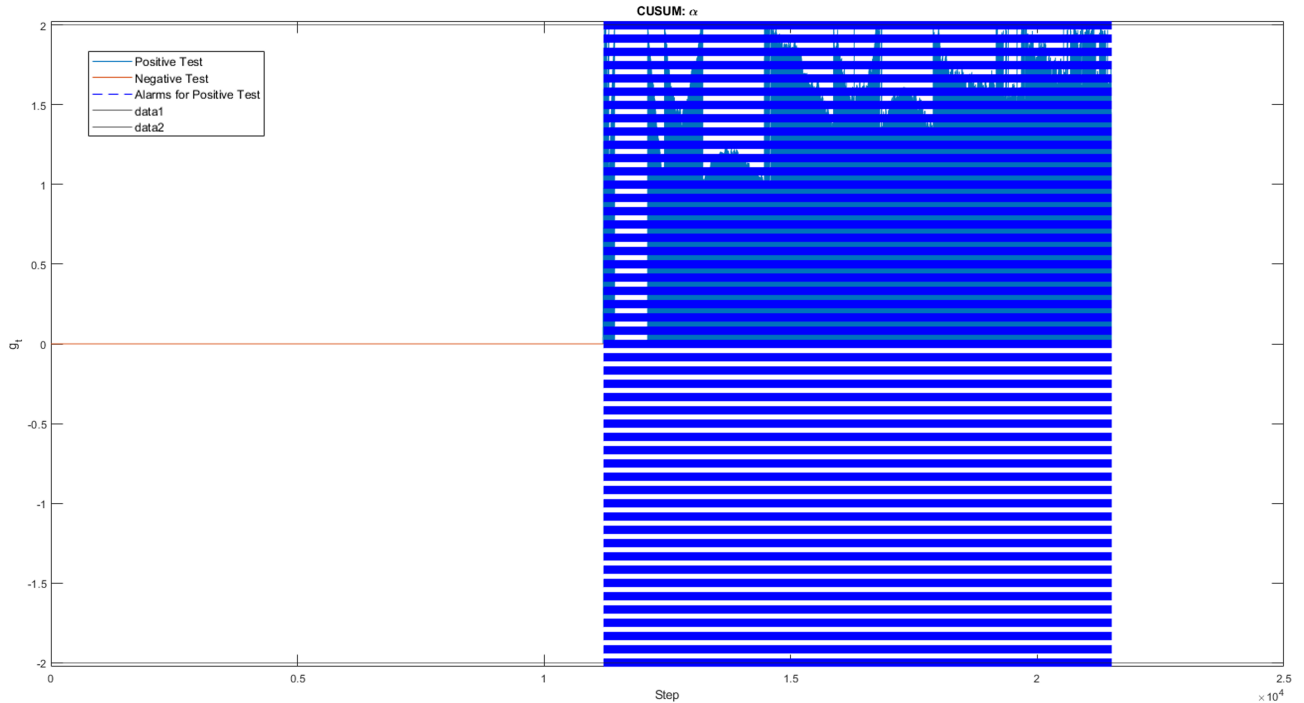


**Figure 11:** Fault Time Instance for Angle of Attack (From CUSUM Test)

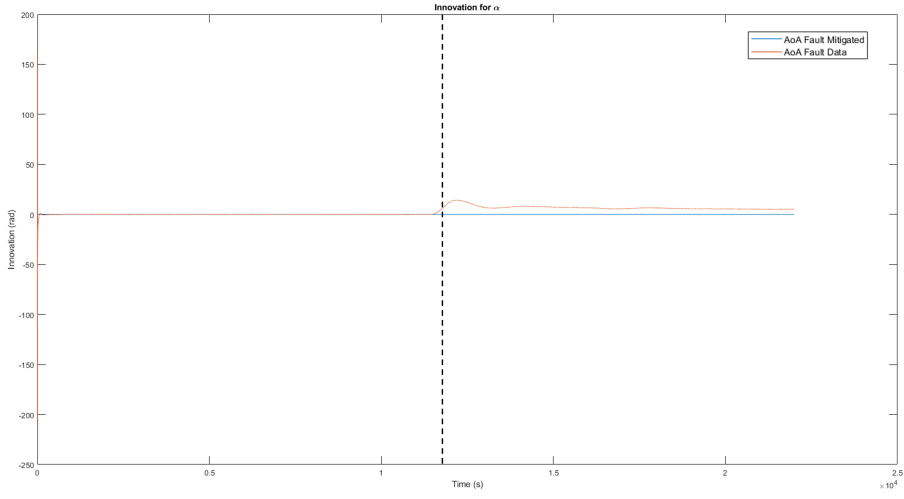


**Figure 12:** Innovation Comparison of AoA with and without Fault Mitigation

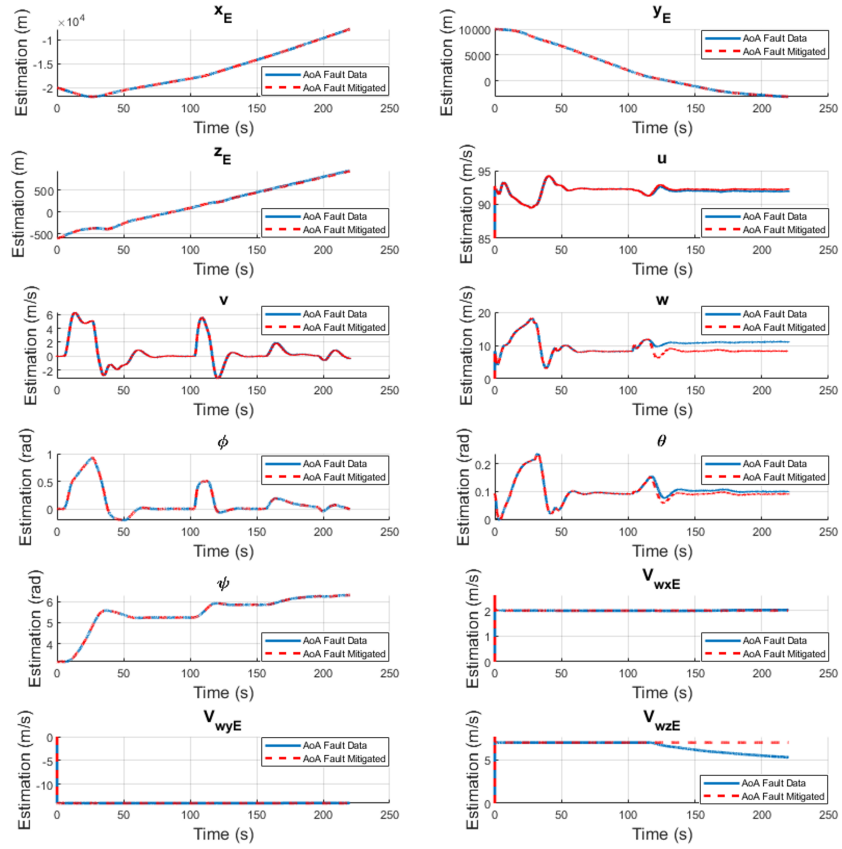


**Figure 13:** Estimated State Trajectories after Cyber Attack Mitigation

## References

- [1] G. Oelsner, V. Schultze, R. IJsselsteijn, F. Wittkämper, and R. Stolz, “Sources of heading errors in optically pumped magnetometers operated in the earth’s magnetic field,” *Physical Review A*, vol. 99, no. 1, p. 013420, 2019.
- [2] A. Lapworth, “Problems in the use of inclinometers and magnetometers to determine translation and orientation of a turbulence probe,” *Journal of Atmospheric and Oceanic Technology*, vol. 12, no. 2, pp. 427–434, 1995.
- [3] A. Lapworth, “Problems in the use of inclinometers and magnetometers to determine translation and orientation of a turbulence probe,” *Journal of Atmospheric and Oceanic Technology*, vol. 12, no. 2, pp. 427 – 434, 1995.
- [4] A. Grant and R. Watkins, “Errors in turbulence measurements with a sonic anemometer,” *Boundary-layer meteorology*, vol. 46, no. 1, pp. 181–194, 1989.
- [5] J. Liu, Z. Zhao, Z. Fang, Y. Li, and L. Du, “Correction of error of airborne anemometers caused by self-excited air turbulence,” *Sensors*, vol. 23, no. 9, 2023.
- [6] T. Nakai and K. Shimoyama, “Ultrasonic anemometer angle of attack errors under turbulent conditions,” *Agricultural and Forest Meteorology*, vol. 162-163, pp. 14–26, 2012.
- [7] J. Kim, J.-G. Lee, G.-I. Jee, and T.-K. Sung, “Compensation of gyroscope errors and gps/dr integration,” in *Proceedings of Position, Location and Navigation Symposium-PLANS’96*, pp. 464–470, IEEE, 1996.
- [8] N. Metni, J.-M. Pflimlin, T. Hamel, and P. Soueres, “Attitude and gyro bias estimation for a flying uav,” in *2005 IEEE/RSJ International Conference on Intelligent Robots and Systems*, pp. 1114–1120, IEEE, 2005.
- [9] Y. Wang and Z. Shi, “Research on cascading effect analysis of civil aircraft inertial reference system parameters failures,” in *Journal of Physics: Conference Series*, vol. 2457, p. 012033, IOP Publishing, 2023.
- [10] U. I. Bhatti and W. Y. Ochieng, “Failure modes and models for integrated gps/ins systems,” *The Journal of Navigation*, vol. 60, no. 2, pp. 327–348, 2007.
- [11] D. M. Bevly and B. Parkinson, “Cascaded kalman filters for accurate estimation of multiple biases, dead-reckoning navigation, and full state feedback control of ground vehicles,” *IEEE Transactions on Control Systems Technology*, vol. 15, no. 2, pp. 199–208, 2007.
- [12] C. K. Chui, G. Chen, *et al.*, *Kalman filtering*. Springer, 2017.
- [13] J.-P. Drécourt, H. Madsen, and D. Rosbjerg, “Bias aware kalman filters: Comparison and improvements,” *Advances in water resources*, vol. 29, no. 5, pp. 707–718, 2006.
- [14] R. Cechowicz, “Bias drift estimation for mems gyroscope used in inertial navigation,” *acta mechanica et automatica*, vol. 11, no. 2, pp. 104–110, 2017.

- [15] W. Gao, Q. Nie, G. Zai, and H. Jia, “Gyroscope drift estimation in tightly-coupled ins/gps navigation system,” in *2007 2nd IEEE Conference on Industrial Electronics and Applications*, pp. 391–396, IEEE, 2007.
- [16] S. Mansoor, U. I. Bhatti, A. I. Bhatti, and S. M. D. Ali, “Improved attitude determination by compensation of gyroscopic drift by use of accelerometers and magnetometers,” *Measurement*, vol. 131, pp. 582–589, 2019.
- [17] T. Kobayashi and D. L. Simon, “Hybrid kalman filter approach for aircraft engine in-flight diagnostics: sensor fault detection case,” in *Turbo Expo: Power for Land, Sea, and Air*, vol. 42371, pp. 745–755, 2006.
- [18] T. Kobayashi and D. L. Simon, “Hybrid kalman filter approach for aircraft engine in-flight diagnostics: Sensor fault detection case,” 2007.
- [19] “What is the kalman filter innovation sequence?.”
- [20] W. Ding, J. Wang, C. Rizos, and D. Kinlyside, “Improving adaptive kalman estimation in gps/ins integration,” *The Journal of Navigation*, vol. 60, no. 3, pp. 517–529, 2007.
- [21] X. ZhiWen, H. XiaoPing, and L. JunXiang, “Robust innovation-based adaptive kalman filter for ins/gps land navigation,” in *2013 Chinese Automation Congress*, pp. 374–379, IEEE, 2013.
- [22] P. B. Dao, “A cusum-based approach for condition monitoring and fault diagnosis of wind turbines,” *Energies*, vol. 14, no. 11, p. 3236, 2021.
- [23] A. Saghaei, M. Mehrjoo, and A. Amiri, “A cusum-based method for monitoring simple linear profiles,” *The International Journal of Advanced Manufacturing Technology*, vol. 45, pp. 1252–1260, 2009.